Available online at www.sciencedirect.com
ScienceDirect
Journal of Hazardous Materials 150 (2008) 587–595
Journal of Hazardous Materials
www.elsevier.com/locate/jhazmat

Use of clinoptilolite for the removal of nickel ions from water: Kinetics and thermodynamics

Mehmet Emin Argun *

Department of Environmental Engineering, Engineering & Architecture Faculty, Selçuk University, 42003 Selçuklu-Konya, Turkey

Received 17 January 2007; received in revised form 3 May 2007; accepted 4 May 2007
Available online 10 May 2007

Abstract

This paper describes the removal of Ni(II) ions from aqueous solutions using clinoptilolite. The effect of clinoptilolite level, contact time, and pH were determined. Different isotherms were also obtained using concentrations of Ni(II) ions ranging from 0.1 to 100 mg L^{-1}. The ion-exchange process follows second-order reaction kinetics and follows the Langmuir isotherm. The paper discusses thermodynamic parameters, including changes in Gibbs free energy, entropy, and enthalpy, for the ion-exchange of Ni(II) on clinoptilolite, and revealed that the ion-exchange process was spontaneous and exothermic under natural conditions. The maximum removal efficiency obtained was 93.6% at pH 7 and with a 45 min contact time (for 25 mg L^{-1} initial concentration and a 15 g L^{-1} solid-to-liquid ratio).

Keywords: Clinoptilolite; Nickel removal; Ion-exchange; Reaction kinetics

1. Introduction

Heavy metal pollution occurs in many industrial wastewater such as those produced by metal-plating facilities, dyeing operations, mining and metallurgical engineering, electroplating, nuclear power plants, aerospace industries, battery manufacturing processes, the production of paints and pigments, glass production, and municipal and storm water runoff. This wastewater commonly includes Ni, Cu, Cd, Cr, and Pb. The effects of Ni exposure vary from skin irritation to damage to the lungs, nervous system, and mucous membranes. It is also known carcinogen. The Turkish discharge standard in wastewater systems for Ni(II) is 5 mg L^{-1} [1]. Therefore, the removal of excess Ni ions from wastewater is essential.

The most widely used methods for removing heavy metals are chemical or electrochemical precipitation, both of which pose a significant problem in terms of disposal of the precipitated wastes [2,3], and ion-exchange treatments, which do not appear to be economical [4]. It has been reported that some aquatic plants [5,6], agricultural byproducts [7–9], sawdust [10], clay [11,12], zeolite [13], turba (partially decomposed vegetable matter) [14,15], and microorganisms [16,17] have the capacity to adsorb and accumulate heavy metals.

Previous research has studied the ion-exchange capacities of titanates such as $K_2Ti_4O_9$ and $Na_2Ti_3O_7$ towards nickel and other ions, and ion-exchange capacities of 156 mg g^{-1} were observed [4]. Although the capacity of these materials is good, the materials are rare in nature, they are toxic, and synthesizing them is expensive. Removal of Ni(II) by the duckweed plant, *Lemna minor*, has also been reported; this plant removed 82% of the Ni in solution [6]. The white-rot fungus *Polyporus versicolor* has also been investigated as a biosorbent for Ni(II) removal. Kinetics and isotherm sorption experiments were conducted to evaluate the effects of pH, time, temperature, and mixing intensity, and the maximum adsorption capacity was 57 mg g^{-1} [16]. The removal of Ni(II) ions from aqueous solutions using acid-modified pine tree materials has been investigated on a laboratory scale, and the maximum adsorption capacities obtained for acid-modified pine bark and pine cones were 20.58 and 1.67 mg g^{-1}, respectively [8]. These types of treatments have the disadvantage of increasing the chemical oxygen demand (COD) of the water. Because of the problems with the aforementioned solutions, it remains necessary to develop a low-cost, easily available material for wastewater treatment that might

* Tel.: +90 332 223 2058; fax: +90 332 241 0635.
E-mail address: argun@selcuk.edu.tr.

0304-3894/$ – see front matter © 2007 Elsevier B.V. All rights reserved.
doi:10.1016/j.jhazmat.2007.05.008

remediate the environmental problems in developing countries. The clay- and zeolite-based ion-exchangers described in this paper have satisfactory ion-exchange capacity and low cost, are abundant in nature, and are not toxic. For example; the retention of Ni(II) by two Portuguese natural ball-clays named ZA-4 and NC and their mineralogical compositions and physical characteristics related to the efficiency of Ni(II) removal were reported by Márquez et al. [12]. The ion-exchange capacities of these clays were 3.6 and 6.5 mg g^{-1}, respectively. Álvarez-Ayuso et al. [13] reported the ion-exchange of Ni(II) with synthetic and natural clinoptilolite and found that exchange capacities were 20.1 and 2 mg g^{-1}, respectively.

Clinoptilolite is one of the most abundant forms of zeolite in Turkey, with a wide geographic distribution and large deposits. The typical formula for natural clinoptilolite is $Na_6[(AlO_2)_6(SiO_2)_{30}]\cdot 24\ H_2O$ [18]. However, the chemical composition of a zeolite is usually variable in both its framework part and the extra-framework cation population. The microporosity and relatively high surface area of zeolites are utilized extensively in applications that require ion-exchangers, adsorbents, catalysts, and separation media [19]. The use of zeolites as ion-exchanger for environmental protection and other applications has been stimulated by good results obtained in testing and by the non-toxic nature of these materials. Clinoptilolite is particularly interesting due to its availability and low cost. The cost of clinoptilolite is negligible (approximately US$0.06–$0.08 kg^{-1}) compared with the cost of activated carbon (US$145 kg^{-1}; Charcoal, Activated Coconut, EMD Chemicals) and ion-exchange resins (US$390 kg^{-1}; Dowex(r) 50WX8-100 ion-exchange resin) [20].

The present paper discusses the efficiency of clinoptilolite for removing Ni(II), which is known to be one of the major contaminants of the water at many sites around the world.

2. Materials and methods

2.1. Adsorbents and reagents

We obtained clinoptilolite from natural zeolites extracted from deposits at Manisa (Turkey). In accordance with ASTM Method D4749 [21], crushed particles were sieved through a range of sieves, and only the particles that passed through a 0.42-mm mesh were used in this study. The sieves were shaken for approximately 15 min, then the separated particles were stored. The zeolite materials were washed with distilled water three times to avoid any effects from dissolved salts in the equilibrium solution. The adsorbents were then oven-dried at 85 °C for 2 h. In our study, an initial Ni(II) concentration of 25 mg L^{-1} was selected because the Ni(II) concentration in the wastewater of three metal-plating companies was about this concentration (19.4, 25, and 26 mg L^{-1}; M.E. Argun, Selçuk University, unpublished data). A stock solution of Ni(II) (1000 mg L^{-1}) was prepared by dissolving a weighed quantity of $NiCl_2$ salts in twice-distilled water. The stock solution was then used to prepare solutions with Ni(II) concentrations ranging from 0.1 to 100 mg L^{-1}. Before adding the adsorbents, the pH of each solution was adjusted to the required value by adding 0.1 M NaOH or 0.1 M HNO_3. Furthermore a background electrolyte has not been added during the ion-exchange experiments. All the chemical compounds used to prepare the reagent solutions were of analytic grade (Merck, Whitehouse Station, NJ).

2.2. Instruments

The chemical compositions of the zeolite samples were determined using a Rigaku RIX 3000 X-ray spectrometer according to the Rietveld method [22]. Infrared spectra of clinoptilolite in solid phase were performed using a Fourier transform infrared spectrometer (Spectrum 2000 Explorer, Perkın-Elmer, USA). Zeta potential measurements were conducted using a zetameter (Nano ZS, Malvern Inst., UK) equipped with a microprocessor unit. The unit automatically calculates the electrophoretic mobility of the particles and converts it to the zeta potential using the Smoluchowski equation [23]. The surface area of the clinoptilolite was measured by "three point" N_2 gas adsorption method using Quantachrome surface analyzer (Model Autosorb-1, Boynton. Beach, FL). A Gallenkamp thermal stirrer was used for the batch experiments. The metal solution was filtered through 0.45-μm membrane filters after settling. It was then analyzed using a Varian inductively coupled plasma-atomic emission spectrometer (Vista AX CCD Simultaneous ICP-AES, Varian, Australia). The pH measurements were performed with digital ion analyzer with a combination electrode (Multi 340i, WTW, Weilheim, Germany).

2.3. Batch sorption experiments and model equations

The metal concentration in the liquid phase was determined at the beginning (C_o) and end (C_e) of the agitation. The following equation was used to compute the percentage uptake of the metal by the clinoptilolite:

$$\text{Sorption}\% = \frac{[(C_o - C_e) \times 100]}{C_o} \quad \text{(i)}$$

The data obtained were applied to the Langmuir isotherm using the following linear expression of this model [24]:

$$\left(\frac{C_e}{q_e}\right) = \left(\frac{1}{bK}\right) + \left(\frac{C_e}{b}\right) \quad \text{(ii)}$$

where q_e is the amount of Ni(II) ions-exchanged per unit weight of clinoptilolite at the equilibrium (mg g^{-1}) and is expressed as $q_e = [(C_o - C_e)V]/M$; V (L) is the volume of the solution; M (g) the amount of clinoptilolite added to the solution; C_e (mg L^{-1}) the metal concentration in the aqueous phase; and b (mg g^{-1}) and K (L mg^{-1}) are the Langmuir constants related to the ion-exchange capacity and energy of ion-exchange, respectively.

Another isotherm, the Dubinin–Radushkevich (D–R) isotherm, was calculated from the ion-exchange data. This isotherm is more general than the Langmuir isotherm since it does not assume a homogeneous surface or constant sorption potential. The D–R equation is expressed as follows [25]:

$$q_e = X'_m \exp(-K'\varepsilon^2) \quad \text{(iii)}$$

Table 1
Experimental conditions for the ion-exchange of Ni(II) on the clinoptilolite

	Ms (g L^{-1})	t (min)	pH	Co (mg L^{-1})	S (rpm)
Effect of clinoptilolite mass, Ms (g)	0.5–30	60	6	25	250
Effect of contact time, t (h)	15	0–200	6	25	250
Effect of pH	15	45	2–9	25	250
Effect of metal concentration, Co (mg L^{-1})	15	180	7	0.1–100	250

where ε (the Polanyi potential) $= RT\ln(1 + 1/C_e)$, q_e and C_e are described under Eq. (ii) (mg g^{-1} and mg L^{-1}, respectively), X'_m is the maximum ion-exchange capacity of the clinoptilolite (mg g^{-1}), K' is a constant related to the ion-exchange energy (mol^2 kJ^{-2}), R the gas constant (kJ K^{-1} mol^{-1}), and T is the temperature (K). The D–R isotherm can be expressed in linear form as follows:

$$\ln q_e = \ln X'_m - K'\varepsilon^2 \quad \text{(iv)}$$

The Freundlich isotherm was also applied to the ion-exchange data. This model has the following linear expression [26]:

$$\log q_e = \log K_f + \left(\frac{1}{n}\right) \log C_e \quad \text{(v)}$$

where K_f (mg g^{-1}) is the Freundlich constant related to the ion-exchange capacity of the sorbent, and $1/n$ is the Freundlich constant related to the energy heterogeneity of the system and the size of the exchanged molecule.

The kinetic parameters for the ion-exchange process were studied for the trial of ion-exchange at 25 mg L^{-1} of Ni(II) at 293 K and pH 7. The contact time was varied between 1 and 200 min and the percent removal of Ni(II) was monitored. The pseudo-first order ([27]; Eq. (vi)) and pseudo-second order ([15]; Eq. (vii)]) kinetic models were selected to test the ion-exchange dynamics in this work because of their good applicability in most cases in comparison with the first and second order models:

$$\log(q_e - q_t) = (\log q_e) - k_1 t \quad \text{(vi)}$$

$$\frac{t}{q_t} = \frac{1}{k_2 q_e^2} + \left(\frac{1}{q_e}\right) t \quad \text{(vii)}$$

where q_t is the amount of Ni(II) removed at the time t (mg g^{-1}), and k_1 (min^{-1}) and k_2 (g mg^{-1} min^{-1}) are the rate constants of the first- and second-order kinetic equations for ion-exchange.

Film and pore diffusion equations (Eq. (viii) and Eq.(ix), respectively) were used to check whether diffusion step controlled to ion exchange process or not [28]:

$$D_f = 0.23\frac{r_0 \delta q_e}{t_{1/2}} \quad \text{(viii)}$$

$$D_p = \frac{0.03 r_0^2}{t_{1/2}} \quad \text{(ix)}$$

where D_f is the film diffusion coefficient (cm^2 s^{-1}), D_p the pore diffusion coefficient (cm^2 s^{-1}), r_0 the radius of clinoptilolite (0.01 cm), δ the film thickness (cm), q_e the equilibrium loading of the clinoptilolite (mg g^{-1}) and $t_{1/2}$ is the half time for the ion-exchange process (min). These equations have been applied to describe the kinetics of several sorption systems [28,29], and the film thickness is taken as 10^{-3} cm assuming geometry of the spherical particles.

The changes in Gibbs free energy (ΔG), enthalpy (ΔH), and entropy (ΔS) for the ion-exchange process were obtained using the following equations [30]:

$$\Delta G = -RT \ln b \quad \text{(x)}$$

$$\ln b = \left(\frac{\Delta S}{R}\right) - \left(\frac{\Delta H}{RT}\right) \quad \text{(xi)}$$

The enthalpy change (ΔH) and the entropy change (ΔS) can be calculated from a plot of ln b (Langmuir constant) versus $1/T$.

2.4. General procedures

We studied the effects of clinoptilolite mass, contact time, pH, and initial metal ion concentration on the exchange of Ni(II) ions using the experimental conditions shown in Table 1. The ion-exchange experiments were performed in a batch reactor using stoppered Pyrex glass flasks.

Each experiment was replicated three times, and the mean values were used in our analyses. If the standard errors (SE) were greater than 0.01, the test was repeated to control for errors. The deviation of the metal uptake per unit weight of clinoptilolite (Δq_e) was calculated as follows:

$$\Delta q_e(\%) = \frac{\sum_{i=1}^{N} |[(q_e)_{cal} - (q_e)_{exp}]/(q_e)_{exp}|}{N} \times 100 \quad \text{(xii)}$$

where the subscripts "exp" and "cal" show the experimental and calculated values of q_e and N is the number of measurements.

Table 2
The chemical composition of Manisa (Turkey) clinoptilolite used in the present study (wt%)

	SiO_2	Al_2O_3	CaO	K_2O	Na_2O	Fe_2O_3	MgO	Loss on ignition (*LoI*)
Coarse grains	68.96	12.45	2.53	3.52	1.34	0.82	1.40	8.98
Fine grains	69.12	12.05	2.23	3.61	0.32	0.98	1.30	10.39

3. Results and discussion

3.1. Material characterization

3.1.1. Chemical and physical properties

The chemical composition of the natural clinoptilolite is presented in Table 2. According to the chemical analysis the theoretical ion exchange capacity is 5.57 ± 0.15 mequiv. g^{-1}. This capacity is the result of the presence of cations such as Na, Ca, Mg and K which are considered to be exchangeable. The Manisa zeolite had the following properties: 1.9–2.2 mequiv. g^{-1} (56–62 mg g^{-1}) of cation-exchange capacity (CEC; i.e., the capacity to adsorb exchangeable cations), 0.40-nm pore diameter, 40% bed porosity, a solid density of 2.15 g cm^{-3}, and a bulk density of 1.30 g cm^{-3} [31]. The surface area was 12 m^2 g^{-1} as measured using the BET (Brauner Emmett Teller) method with nitrogen gas.

3.1.2. Functional groups

The evaluation of the FT-IR spectra of clinoptilolite was summarized in Table 3. It should be noticed that the higher percentages of transmittance mean the lower amount of functional groups. Table 3 presents the fundamental frequencies of clinoptilolite before and after Ni(II) exchange, and their respective possible assignments in the FT-IR spectrum [32]. FT-IR spectrums also show that clinoptilolite constituents mainly composed of Si–O(H)–Si, Si–O(H)–Al, Si–O–Si and Si–O–Al groups. It has been known that all these groups have affinity of heavy metal adsorption [33]. It could be concluded from Table 3 that all functional groups, which increase ion-exchange capacity, decreased after Ni(II) exchange. This could be resulted from that Ni(II) ions captured functional groups of zeolite.

3.1.3. Zeta-potential

The zeta potential measurements were carried out as a function of pH with the relation of electrophoretic mobility of the particles. From the Fig. 1 it was concluded that the zeta potential of clinoptilolite was strongly affected from the pH of the metal solution. Under acidic conditions, the clinoptilolite mineral surface was covered with H^+ ions and zeta-potential decreased to −13 mV. However, with increasing pH, the hydroxyl ions increased on the clinoptilolite surface and the zeta-potential increased to −51 mV for pH 13. In other words, the clinoptilolite surface has a negative charge for all pH from 2 to 13 and the clinoptilolite could adsorb heavymetal ions even in low pH solution and can be applied for actual strong acidic wastewater. The negative charge results from the Al^{3+} substitutions for Si^{4+} within the clinoptilolite lattice (isomorphic substitution), the broken bonds at the Si–O–Si generated at the particle surface during the grinding process and the lattice imperfections [18,34].

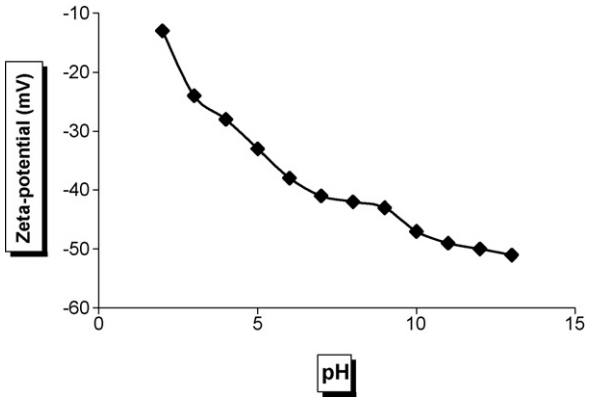

Fig. 1. The variation of the zeta potential of clinoptilolite vs. pH.

3.2. Effect of operational condition

3.2.1. Effect of the mass of clinoptilolite

The effect of the mass of clinoptilolite on the retention of Ni(II) was studied using 100 mL of 25 mg L^{-1} Ni(II) solution treated with 0.5 to 3.0 g of clinoptilolite for 60 min. Fig. 2 shows that the Ni(II) retention increased gradually with increasing mass of clinoptilolite to a mass of 15 g L^{-1}. This clinoptilolite dosage decreased the Ni(II) concentration to 1.8 mg L^{-1}, which is less than the discharge limit (5 mg L^{-1}) for wastewater. After this clinoptilolite concentration, the removal efficiency of Ni(II) increased by only 0.95% with increased clinoptilolite mass. Thus, *I* used this concentration for the following experiments. These results suggested that the proportional increase between clinoptilolite dosage and removal efficiency was related to an increase in the number of ion-exchange sites

Table 3
Fundamental FT-IR spectra of natural clinoptilolite before and after Ni(II)-exchange

Before exchange		After exchange		Possible assignments
BP (cm^{-1})[a]	T (%)[b]	BP (cm^{-1})[a]	T (%)[b]	
3614	3,195	–	–	Surface hydroxyl groups (Si–OH–Si, or Al–OH–Al)
3462	2,974	3351	31,917	Stretching vibration of adsorbed water molecules
2363	11,40	2284	37,371	Calcite and dolomite
1638	3,964	1738	36,325	Bending vibration of adsorbed water
1052	0,107	1034	17,303	Si–O stretching vibration of quartz
791	5,629	898	31,581	Si–O stretching vibration of quartz
721	6,155	831	33,372	The characteristic band of calcite
603	1,925	603	23,355	Si–O–Al and Si–O–Si bending vibrations

[a] Band positions.
[b] Transmittance.

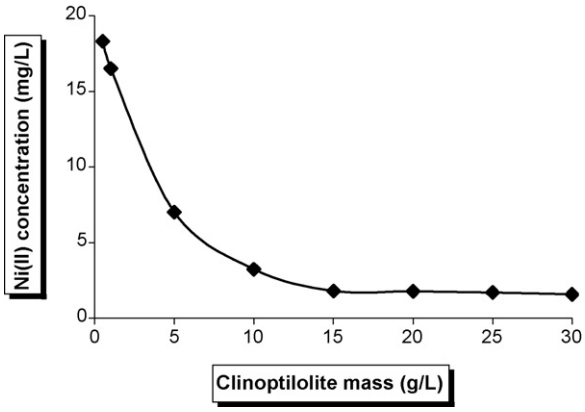

Fig. 2. Effect of the mass of clinoptilolite on the removal of Ni(II). The initial concentration of Ni(II) was 25 mg L^{-1}, the agitation speed was 250 rpm, the contact time was 60 min, and the temperature was 293 K.

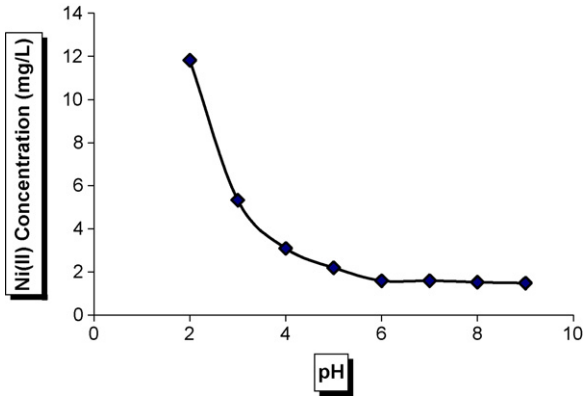

Fig. 4. Effect of pH on the removal of Ni. The initial concentration of Ni(II) was 25 mg L^{-1}, the clinoptilolite concentration was 15 g L^{-1}, the agitation speed was 250 rpm, the contact time was 45 min, and the temperature was 293 K.

3.2.2. *Effect of contact time*

The removal of Ni(II) as a function of contact time is shown in Fig. 3. Because shaking consumes energy, and the cost increases with increasing shaking time, it is important to determine the suitable contact time that maximizes removal efficiency without unacceptably increasing the cost. The graph shows that the ion-exchange efficiency initially increased rapidly and the equilibrium was attained in 180 min at adsorption efficiency of 97%. Although the highest value of exchanged Ni(II) ions by clinoptilolite was reached at 180 min there was no big difference between obtained data for 45 min (93%) and 180 min. Consequently, a contact time of 45 min was chosen for the pH and regeneration experiments. For isotherm experiments 180 min contact time was chosen because of the equilibrium time is more important. The removal efficiency decreased by only about 0.02% after equilibrium had been reached. This probably resulted from saturation of adsorbent surfaces with heavy metals followed by adsorption and desorption processes that occur after saturation.

3.2.3. *Effect of pH*

The effect of pH on the ion-exchange of Ni(II) by the clinoptilolite is presented in Fig. 4. The pH of the aqueous solution was an important parameter that controlled the ion-exchange process. Ion-exchange increased with increasing pH to a pH of around 6, then increased only slowly thereafter, with further pH increases resulting in precipitation. At pH lower than 8, Ni(II) ions were the dominant species; $Ni(OH)_2$ was present at pH higher than 8 [35]. Under acidic conditions, the clinoptilolite mineral surface will be completely covered with H^+ ions and the Ni(II) ions cannot compete with them for ion-exchange sites. However, with increasing pH, the competition from the hydrogen ions decreases and the positively charged Ni(II) ions can be exchanged with exchangeable cations and can also be adsorbed at the negatively charged sites on the clinoptilolite [36]. Based on these results, clinoptilolite exhibited a good capacity for removing Ni(II) from solution at a range of pH values from 6 to 9. The maximum ion-exchange (1.6 mg g^{-1} and 93.6%) was at a pH of 7 with a 45-min contact time, a 15 g L^{-1} solid-to-liquid ratio, and an initial heavy metal concentration of 25 mg L^{-1}.

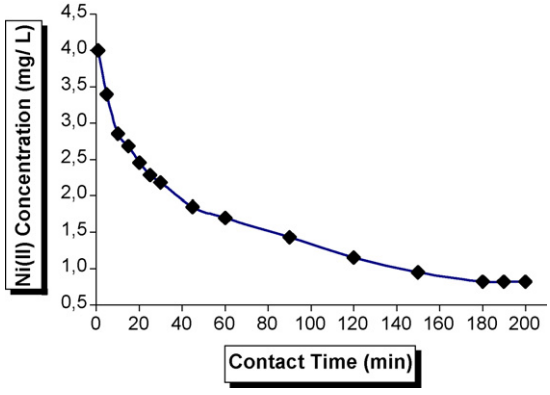

Fig. 3. Effect of contact time on the removal of Ni(II). The initial concentration of Ni(II) was 25 mg L^{-1}, the clinoptilolite concentration was 15 g L^{-1}, the agitation speed was 250 rpm, and the temperature was 293 K.

3.3. *Determination of ion-exchange isotherms*

Ion-exchange isotherms or capacity studies are of fundamental importance in the design of ion-exchange systems since they indicate how the metal ions are partitioned between the adsorbent and liquid phases at equilibrium as a function of increasing metal concentration. When an adsorbent and metal ion solution is placed in contact, the concentration of metal ions on the adsorbent will increase until a dynamic equilibrium is reached; at this point, there is a defined distribution of metal ions between the solid and liquid phases. The Ni-exchange capacities at pH 7 were calculated by means of least-squares regression using Eqs. (ii), (iv) and (v). The resulting isotherms for the clinoptilolite used in this study are shown in Figs. 5–8.

The regression values and correlation coefficients (R^2) presented in Table 4 indicate that the ion-exchange data for Ni(II) removal best fitted the Langmuir isotherm. However, the D–R and Freundlich isotherms are important because they do not assume a homogeneous surface. At 293 K, the ion-exchange capacity b (Langmuir isotherm) was 3.28 mg g^{-1} and the ion-exchange capacity X'_m (D–R isotherm) and K_f were 1.81 mg g^{-1} and 0.68 mg g^{-1}, respectively. The maximum ion-exchange

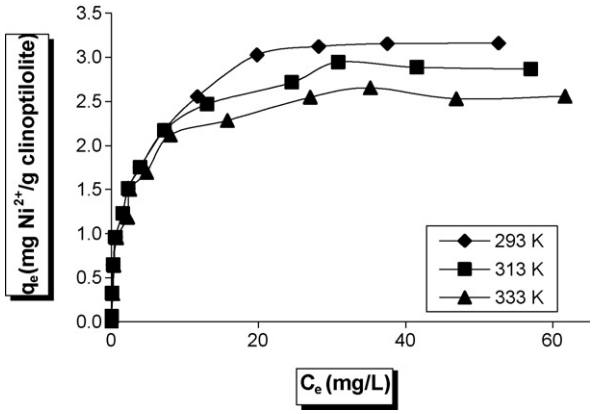

Fig. 5. Ion-exchange isotherm for clinoptilolite using different initial Ni concentrations ranging from 0.1 to 100 mg Ni(II) L^{-1}. The clinoptilolite concentration was 15 g L^{-1}, and the contact time was 180 min at pH 7.

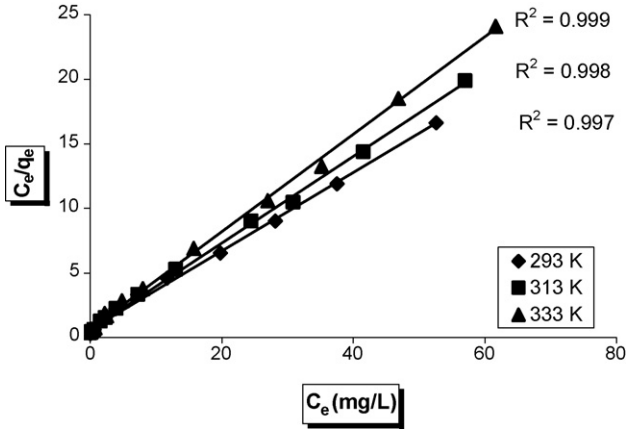

Fig. 6. The linearized Langmuir isotherm for ion-exchange of Ni(II) by clinoptilolite. The clinoptilolite concentration was 15 g L^{-1}, and the contact time was 180 min at pH 7.

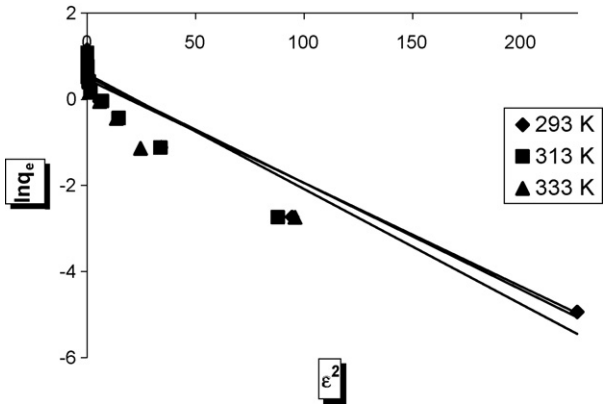

Fig. 7. The linearized D–R isotherm for ion-exchange of Ni(II) by clinoptilolite.

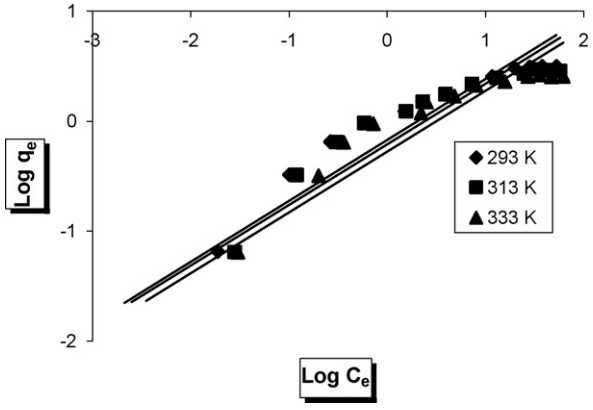

Fig. 8. The linearized Freundlich isotherm for ion-exchange of Ni(II) by clinoptilolite. The clinoptilolite concentration was 15 g L^{-1}, and the contact time was 180 min at pH 7.

capacity based on the Langmuir isotherm (3.3 mg g^{-1}) is lower then the CEC (56–62 mg g^{-1}) of clinoptilolite that was reported by Benkli et al. [31]. This could occur if the uptake of Ni(II) ions on the clinoptilolite surface forms a monolayer more often than it forms a bilayer and if the electron configuration of Ni(II) ions prevents a greater uptake capacity. It is also possible that the ion-exchange occurs as a result of the interaction between nickel ions and specific ions in the material's cation-exchange site. However, all cation-exchange sites are less common usable due to variable framework of clinoptilolite in a real-world solution, thus ion exchange would more often require the replacement of an adsorbed charged species by another charged species from the surrounding solution. In addition, increasing the initial Ni concentration in the solution decreased the removal efficiency. This may be due to a progressive decrease in the proportion of covalent interactions and an increase in the proportion of electrostatic interactions at sites with a lower affinity for Ni(II) as the initial Ni(II) concentration increased.

3.4. Determination of ion-exchange kinetics

In order to determine the ion-exchange kinetics of Ni(II), the pseudo-first-order and pseudo-second-order kinetics models were examined. The slopes and intercepts of these curves were used to determine the pseudo-first-order and pseudo-second-order constants k_1 and k_2 and the equilibrium capacity q_e. The

Table 4
The Langmuir, D–R, and Freundlich constants and correlation coefficients of isotherm models at different temperature

Temperature (K)	Langmuir Isotherm			D-R Isotherm			Freundlich Isotherm		
	b	K	R^2	X'_m	K'	R^2	$1/n$	K_f	R^2
293	3.28	0.182	0.996	1.81	0.027	0.909	0.553	0.676	0.911
313	2.97	0.194	0.997	1.69	0.025	0.896	0.551	0.619	0.894
333	2.65	0.249	0.995	1.58	0.024	0.901	0.553	0.532	0.886

(Ni(II) concentration: 0.1–100 mg L^{-1}, clinoptilolite dosage: 15 g L^{-1}, agitation speed: 250 rpm, and contact time: 180 min at pH 7).

Table 5
The kinetics constants for the exchange of Ni(II) ions on the clinoptilolite

T (K)	$(q_e)_{exp}$ (mg g^{-1})	Pseudo-first-order kinetics			Pseudo-second-order kinetics			Film diffusion, D_f (cm^2 s^{-1})	Pore diffusion, D_p (cm^2 s^{-1})
		$(q_e)_{cal}$ (mg g^{-1})	k_1 (min^{-1})	Δq_e (%)	$(q_e)_{cal}$ (mg g^{-1})	k_2 (g mg^{-1} min^{-1})	Δq_e (%)		
293	1.61	0.174	0.0081	89	1.60	0.522	0.43	3.1×10^{-9}	2.5×10^{-9}
313	1.58	0.15	0.0075	91	1.59	0.75	0.63	2.4×10^{-9}	2.3×10^{-9}
333	1.56	0.12	0.0070	92	1.58	1.2	1.3	1.9×10^{-9}	2.0×10^{-9}

(clinoptilolite dosage: 15 g L^{-1}, pH: 7, agitation speed: 250 rpm, particle diameter: 0.2 mm).

calculated (cal) value of q_e (Table 5) from the pseudo-first-order kinetics model was dramatically lower than the experimental (exp) value. However, the pseudo-second-order kinetics model (Fig. 9, Table 5) provided a near-perfect match between the theoretical and experimental q_e values. As a result, the ion-exchange process appears to follow pseudo-second-order reaction kinetics. The pseudo-second-order kinetics model also described the data better than the first-order model ($r^2 = 0.97$ and 0.99, respectively).

The pseudo-second-order kinetic rate constant for Ni(II)-exchange on clinoptilolite was $k_2 = 0.522$ g mg^{-1} min^{-1} (31.32 g mg^{-1} h^{-1}). When the Ni(II) ion solution is mixed with the adsorbent, transport of the Ni(II) ions from the solution through the interface between the solution and the adsorbent and into the particle pores is effective. There are essentially four stages in the process of ion-exchange by porous adsorbents [37]: (i) solute transfer from the bulk solution to the boundary film that borders the exhanger's surface, (ii) solute transport from the boundary film to the exchanger's surface, (iii) solute transfer from the exchanger's surface to active pores of exchanger's, and (iv) interactions between the solute molecules and the available ion-exchange sites on the internal surfaces of the adsorbent.

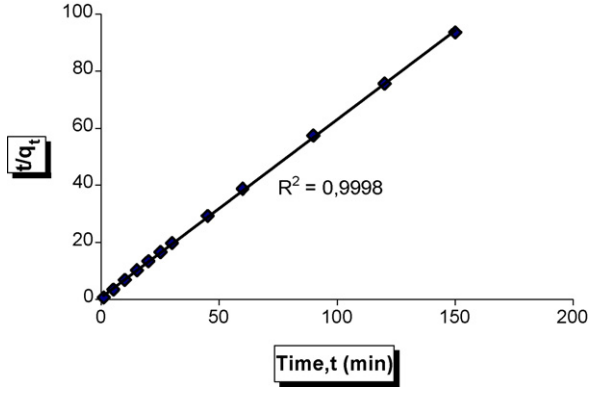

Fig. 9. Linearized pseudo-second-order kinetics plots for ion-exchange of Ni(II) by clinoptilolite (dosage: 15 g L^{-1} at pH 7, shaking speed: 250 rpm, temperature: 293 K).

One or more of these four steps may control the rate at which solute is exchanged. Table 5 depict diffusion of Ni(II) within clinoptilolite as a function of temperature at pH 7. Film and pore diffusion coefficients for 0.2 mm particle diameter were calculated as 3.1 10^{-9} and 2.5 10^{-9} cm^2 s^{-1}, respectively. According to the Michelson et al. [38], D_f values should be in the range of 10^{-6} to 10^{-8} cm^2 s^{-1} for film diffusion to be rate-limiting factor. Similarly, D_p values should be in the range of 10^{-11} to 10^{-13} cm^2 s^{-1} for pore diffusion to be rate-limiting factor. From these results it can be concluded that both of film and pore diffusions are not the rate-limiting step and also confirmed the results mentioned above.

3.5. Effect of temperature and determination of ion-exchange thermodynamics

The temperature dependence of the ion-exchange was calculated by the linearized Arrhenius equation ([39]; Eq. (xiii))

$$\ln(k) = \ln(A) - \left(\frac{E_a}{RT}\right) \quad \text{(xiii)}$$

where E_a is the activation energy of the ion-exchange (kJ mol^{-1}), k the rate constant which controls process, A the Arrhenius constant, R the gas constant (8.314 J mol^{-1} K^{-1}), and T is the solution temperature (K). Kinetic sorption processes usually have energies greater than 25–30 kJ mol^{-1} and diffusion sorption processes have energies usually less than 25–30 kJ mol^{-1}, in which no electrons are transferred or shared between the sorbed molecules/ions and the sorbent surface [39]. The activation energy value also gives us information on whether the adsorption is mainly physical or chemical. Nollet et al. [40] suggested that the physisorption process normally had activation energy of 5–40 kJ mol^{-1}, while chemisorption had higher activation energy (40–800 kJ mol^{-1}). The rate constant k_2 listed in Table 5 was applied to estimate the activation energy of the ion-exchange. In this study the value of 32 kJ mol^{-1} for activation energy was obtained from the slope of an $\ln(k_2)$ versus $1/T$ (Table 6). It was concluded from this result that the adsorp-

Table 6
Thermodynamic coefficients for Ni(II)-exchange by clinoptilolite

T (K)	$\ln b$	ΔG (kJ mol^{-1})	ΔS (kJ mol^{-1} K^{-1})	ΔH (kJ mol^{-1})	E_a (kJ mol^{-1})
293	1.188	−2.89			
313	1.089	−2.83	−0.0049	−4.32	32.0
333	0.974	−2.69			

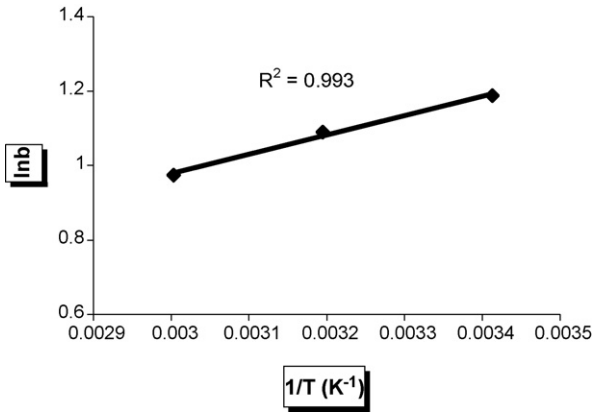

Fig. 10. Plot of the Langmuir constant (ln *b*) vs. temperature (1/*T*). The thermodynamic parameters in Table 6 are determined from this graph.

tion involved physisorption and the process controlled by kinetic sorption. The obtained data from kinetic studies also confirm this result.

The results of the thermodynamic calculations are shown in Table 6. The negative value for the Gibbs free energy shows that the ion-exchange process is spontaneous in nature and that the degree of spontaneity of the reaction decreases with increasing temperature, mainly due to physisorption rather than chemisorption. Fig. 10 also demonstrates that ion-exchange decreases with increasing temperature. The overall ion-exchange process seems to be exothermic ($\Delta H = -4.32\,\mathrm{kJ\,mol^{-1}}$). This result also supports the suggestion that the ion-exchange mechanism is primarily physisorption and that the resulting Ni-exchanger complex is energetically stable. Table 6 also shows that the ΔS values were negative; that is, entropy (randomness) decreased as a result of the ion-exchange. According to the Zou et al. [41] negative value of entropy for removal of Ni on zeolite reflects that no significant change occurs in the internal structure of zeolite.

3.6. Regeneration studies

Regeneration of clinoptilolite is an important step in order to make the ion-exchange process more economical. The regeneration efficiency for clinoptilolite at different eluent solutions of 0.1 M HCl, 0.1 M NaOH, and distilled water are shown in Table 7. Recovery of the exchanged Ni(II) ions and repeated usability of the exchanger is important in reference to the industrial applications. In order to demonstrate the reusability of the clinoptilolite, the adsorption–desorption (A/D) cycles of Ni(II) were repeated three times by using the same clinoptilolite (Table 7). Nearly 96% of the exchanged Ni(II) ions were desorbed from clinoptilolite by using 0.1 M HCl. When HCl was used as a desorption agent, the clinoptilolite mineral surface was completely covered with H^+ ions while the coordination spheres of chelated Ni(II) ions was disrupted. Thereafter the Ni(II) ions could not compete with H^+ ions for ion-exchange sites and subsequently heavy metal ions were released from the solid surface into the solution. Also it was observed a little change on the clinoptilolite structure under these acidic conditions (pH ∼1). For this reason, clinoptilolite regeneration efficiencies and Ni(II) recovery efficiencies were decreased a little from 93% to 80% and from 96% to 85%, respectively. However, under basic conditions, negatively charged surface adsorbed Ni(II) ions instead of desorption. After regeneration desorbed Ni(II) ions were low while Ni(II) uptake efficiency of regenerated clinoptilolite was a litle high because of negatively charged surface. Therefore clinoptilolite regeneration efficiency partially high then Ni(II) recovery efficiency for NaOH regeneration. The results showed that clinoptilolite could be repeatedly used in ion-exchange studies of Ni(II) with slight losses in their initial ion-exchange capacities.

Table 7
Effect of different eluents on regeneration and metal recovery efficiency during repeated adsorption/desoprtion (A/D) cycles (contact time: 45 min, pH: 7, *T*: 298 K)

Eluents	A/D cycle	Clinoptilolite regeneration efficiency (%)[a]	Ni(II) recovery efficiency (%)[b]
0.1 M HCl	1	93	96
	2	88	93
	3	80	85
0.1 M NaOH	1	60	50
	2	55	40
	3	40	20
Distilled water	1	65	68
	2	52	58
	3	45	50

[a] Clinoptilolite regeneration efficiency = (regenerated exchange capacity/original exchange capacity) × 100%.
[b] Ni(II) recovery efficiency = (amount of Ni(II) recovered/amount of Ni(II) exchanged) × 100%.

4. Conclusions

This paper presents the results of a detailed study of equilibrium and kinetics of the ion-exchange process for removing Ni(II) ions from aqueous solution using a common, naturally occurring clinoptilolite. In all experiments clinoptilolite decreased the Ni(II) concentration under the discharge limit ($5\,\mathrm{mg\,L^{-1}}$) for wastewater. However, in an industrial application, the presence of other cations in the wastewater would interfere with the ion-exchange of Ni (II), and would thus decrease the removal efficiency for this specific cation. This is likely to be an acceptable tradeoff if a significant proportion of the other cations are also toxic and must be removed from the wastewater. Operational parameters such as the amount of clinoptilolite, contact time, initial Ni(II) concentrations, and pH of the solution clearly affect the removal efficiency. The optimum Ni(II) removal by the clinoptilolite was obtained at pH 7. The Langmuir, D–R, and Freundlich isotherms could all be used to model isothermal ion-exchange of Ni(II) on clinoptilolite, and the kinetics data could be modeled by a pseudo-second-order kinetics equation. The ion-exchange process was thermodynamically spontaneous under natural conditions.

These results suggest that the capacity of clinoptilolite to exchange certain metal can be calculated using the models described in this paper. The ion-exchange capacity of the clinop-

tilolite for Ni(II) equaled 3.28 mg g^{-1} and the ion-exchange rate (k_2) was 0.522 g mg^{-1} min^{-1}.

Acknowledgments

I thank the Selçuk University Research Fund (BAP) for providing financial support of the work described in this paper. I also would like to thank Mr. Geoff Hart for his assistance in editing this paper.

References

[1] Anon., Turkish water pollution control regulations. Republic of Turkey Ministry of Environment and Forestry. Turkish Official Gazette. Issue: 25687, 2004.
[2] C.L. Lai, S.H. Lin, Electrocoagulation of chemical mechanical polishing (CMP) wastewater from semiconductor fabrication, Chem. Eng. J. 95 (2003) 205–211.
[3] C. Özdemir, M. Karatas, S. Dursun, M.E. Argun, S. Dogan, Effect of $MnSO_4$ on the chromium removal from leather industry wastewater, Environ. Technol. 26 (2005) 397–400.
[4] V.A. Cardoso, A.G. de Souza, P.P.C. Sartoratto, L.M. Nunes, The ionic exchange process of cobalt, nickel and copper(II) in alkaline and acid-layered titanates, Colloid Surface A: Physicochem. Eng. Aspects 248 (2004) 145–149.
[5] B. Volesky, J. Weber, J.M. Park, Continuous-flow metal biosorption in a regenerable *Sargassum* column, Water Res. 37 (2003) 297–306.
[6] N.R. Axtell, S.P.K. Sternberg, K. Claussen, Lead and nickel removal using *Microspora* and *Lemna minor*, Bioresour. Technol. 89 (2003) 41–48.
[7] M.E. Argun, Ş. Dursun, Removal of heavy metal ions using chemically modified adsorbents, J. Int. Environ. Appl. Sci. 1 (2006) 27–40.
[8] M.E. Argun, Ş. Dursun, K. Gür, C. Özdemir, M. Karatas, S. Dogan, Nickel adsorption on the modified pine tree materials, Environ. Technol. 26 (2005) 479–488.
[9] S. Ricordel, S. Taha, I. Cisse, G. Dorange, Heavy metals removal by adsorption onto peanut husks carbon: characterization, kinetic study and modelling, Sep. Purif. Technol. 24 (2001) 389–401.
[10] M.E. Argun, Ş. Dursun, C. Özdemir, M. Karataş, Heavy metal adsorption by oak sawdust: thermodynamics and kinetics, J. Hazard. Mater. 141 (2007) 77–85.
[11] T. Viraraghavan, A. Kapoor, Adsorption of mercury from wastewater by bentonite, Appl. Clay Sci. 9 (1994) 31–49.
[12] G.E. Márquez, M.J.P. Ribeiro, J.M. Ventura, J.A. Labrincha, Removal of nickel from aqueous solutions by clay-based beds, Ceram. Int. 30 (2004) 111–119.
[13] E. Álvarez-Ayuso, A. Garcia-Sánchez, X. Querol, Purification of metal electroplating waste waters using zeolites, Water Res. 37 (2003) 4855–4862.
[14] I. Twardowska, J. Kyziol, Sorption of metals onto natural organic matter as a function of complexation and adsorbent–adsorbate contact mode, J. Environ. Int. 28 (2003) 783–791.
[15] Y.S. Ho, D.A.J. Wase, C.F. Forster, Batch nickel removal from aqueous solution by sphagnum moss peat, Water Res. 29 (1995) 1327–1332.
[16] F.B. Dilek, A. Erbay, U. Yetis, Ni(II) biosorption by *Polyporous versicolor*, Process Biochem. 37 (2002) 723–726.
[17] Q. Li, S. Wu, G. Liu, X. Liao, X. Deng, D. Sun, Y. Hu, Y. Huang, Simultaneous biosorption of cadmium (II) and lead (II) ions by pretreated biomass of *Phanerochaete chrysosporium*, Sep. Purif. Technol. 34 (2004) 135–142.
[18] D.W. Breck, Zeolite Molecular Sieves: Structure, Chemistry and Use, J. Wiley & Sons Inc., New York, 1974.
[19] R. Petrus, J.K. Warchol, Heavy metal removal by clinoptilolite. An equilibrium study in multi-component systems, Water Res. 39 (2005) 819–830.
[20] https://www1.fishersci.com.
[21] American Society for Testing and Materials, Method D4749, 1994.
[22] H.M. Rietveld, A profile refinement method for nuclear and magnetic structures, J. Appl. Cryst. 2 (1969) 65–71.
[23] M. Alkan, Ö. Demirbaş, M. Doğan, Electrokinetic properties of sepiolite suspensions in different electrolyte media, J. Colloid Interf. Sci. 281 (2005) 240–248.
[24] O. Altin, H.O. Ozbelge, T. Dogu, Use of general purpose adsorption isotherms for heavy metal-clay mineral interactions, J. Colloid Interf. Sci. 198 (1998) 130–140.
[25] B.P. Bering, M.M. Dubinin, V.V. Serpinsky, On thermodynamics of adsorption in micropores, J. Colloid Interf. Sci. 38 (1972) 185–194.
[26] S. Balci, Nature of ammonium ion adsorption by sepiolite: analysis of equilibrium data with several isotherms, Water Res. 38 (2004) 1129–1138.
[27] C. Namasivayam, R.T. Yamuna, Adsorption of chromium (VI) by a low-cost adsorbent: biogas residual slurry, Chemosphere 30 (1995) 561–578.
[28] T.S. Anirudhan, M. Ramachandran, Adsorptive removal of tannin from aqueous solutions by cationic surfactant-modified bentonite clay, J. Colloid Interf. Sci. 299 (2006) 116–124.
[29] D.D. Duong, Adsorption Analysis: Equilibria and Kinetics, vol. 2, Imperial College Press, London, 1998.
[30] D. Mohan, K.P. Singh, Single- and multi-component adsorption of cadmium and zinc using activated carbon derived from bagasse: an agricultural waste, Water Res. 36 (2002) 2304–2318.
[31] Y.E. Benkli, M.F. Can, M. Turan, M.S. Çelik, Modification of organo-zeolite surface for the removal of reactive azo dyes in fixed-bed reactors, Water Res. 39 (2005) 487–493.
[32] J. Madejova, FTIR techniques in clay minerals studies: a review, Vib. Spectrosc. 31 (2003) 1–10.
[33] Y.S. Al-Degs, M.I. El-Barghouthi, A.A. Issa, M.A. Khraisheh, G.M. Walker, Sorption of Zn(II), Pb(II), and Co(II) using natural sorbents: equilibrium and kinetic studies, Water Res. 40 (2006) 2645–2658.
[34] J.H.C. Van Hooff, J.W. Roolefson, Introduction to Zeolite Science and Practice: Technics of Zeolite Characterization, Studies in Surface Science and Catalysis, Elsevier, Amsterdam, 1991.
[35] I. Gaballah, G. Kilbertus, Recovery of heavy metal ions through decontamination of synthetic solutions and industrial effluents using modified barks, J. Geochem. Explor. 62 (1998) 241–286.
[36] S.S. Gupta, K.G. Bhattacharyya, Adsorption of Ni(II) on clays, J. Colloid Interf. Sci. 295 (2006) 21–32.
[37] G. McKay, The adsorption of basic dye onto silica from aqueous solution—solid diffusion model, Chem. Eng. Sci. 39 (1984) 129–138.
[38] L.D. Michelson, P.G. Gideon, E.G. Pace, L.H. Kutal, Removal of soluble mercury from wastewater by complexing technique, US Department of Industry, Office of Water Research and Technology, Bull No. 74, 1975.
[39] Y.S. Ho, J.C.Y. Ng, G. McKay, Kinetics of pollutant sorption by biosorbents: review, Sep. Purif. Meth. 29 (2000) 189–232.
[40] H. Nollet, M. Roels, P. Lutgen, P. Meeren, W. Verstraete, Removal of PCBs from wastewater using fly ash, Chemosphere 53 (2003) 655–665.
[41] W. Zou, R. Han, Z. Chen, Z. Jinghua, J. Shi, Kinetic study of adsorption of Cu(II) and Pb(II) from aqueous solutions using manganese oxide coated zeolite in batch mode, Colloid Surface A: Physicochem. Eng. Aspects 279 (2006) 238–246.